Determination of G_E^p/G_M^p in the Nuclear Medium via Recoil Polarization Measurements in the $^{16}O(\vec{e}, e'\vec{p})$ Reaction

R. D. Ransome for the TJNAF Hall A Collaboration

Rutgers University, Piscataway, NJ 08854-8019, USA

Abstract. The first $(\vec{e}, e'\vec{p})$ polarization transfer measurements on a heavy nucleus have been made at TJNAF. The reaction $^{16}O(\vec{e}, e'\vec{p})$ was used to study the transfer of polarization to the recoil proton in quasi-elastic kinematics. The preliminary result for the ratio of longitudinal to transverse polarization is within about 10% of that expected from a standard calculation assuming no change in the nucleon form factor.

1 Introduction

Two fundamental, long standing questions in subatomic physics are *What is the structure of the nucleon?* and *How is that structure changed in the nucleus?* The precise answers to these questions are not known, and much of the effort at the Thomas Jefferson National Accelerator Facility (JLab) is directed toward answering them. In this talk I would like to discuss our work related to the second question.

Many experiments have been performed with the goal of determining if and how the nucleon is modified in the nuclear medium. Different experiments have given different answers and the interpretation of the experiments has changed with time. The measurements are difficult, as are the theoretical calculations required to interpret the data, so on both fronts physicists have been stymied in their efforts to find a convincing conclusion about medium modifications.

Before discussing the current experiment, I would like to briefly mention some of the previous measurements.

The conventional method to extract form factors has been the Rosenbluth separation. The scattering cross section for electron-nucleon scattering can be written as

$$\sigma = \sigma_{mott}\Big(\frac{G_E^2 + \tau G_M^2}{1+\tau} + 2\tau G_M^2 \tan^2(\theta/2)\Big)$$

$$\tau = Q^2/4m_p^2,$$

where σ_{mott} is the Mott scattering cross section, θ is the electron scattering angle, Q^2 is the four momentum transfer squared, m_p the proton mass, and

G_E and G_M the electric and magnetic form factors. This method has the advantage of requiring neither a polarized electron beam nor measurement of the nucleon polarization. It has the disadvantage that it requires measuring an absolute cross section for at least two different angles. Great care needs to be taken to keep systematic errors small, and to correct properly for radiative effects. At larger angles the cross section is dominated by G_M, making a precise measurement of G_E difficult. Experiments to date show no indication of medium modifications [1, 2] at the few percent level for Q^2 up to about 0.3 $(GeV/c)^2$.

The relation between the Coulomb sum, the longitudinal response function of the nucleus, and the effective nucleon charged form factor can be used to determine the modification of the G_E in the nuclear medium [3]. A recent reanalysis of existing data appears to show that the electric form factor does not vary by more than about 4%[4, 5] for Q^2 up to about 0.7 $(GeV/c)^2$.

Another approach has been that of y-scaling, which studies the nuclear response in the quasi-elastic region. Studies of y-scaling[6, 7, 8] have put limits of a few percent on the change of the magnetic form factor for Q^2 up to about 3 $(GeV/c)^2$.

For Q^2 greater than about 1 $(GeV/c)^2$ the ratio of G_E/G_M, even for the proton, is known very poorly, not better than 10%; the uncertainty becomes increasingly larger as Q^2 increases due to the difficulty of using the Rosenbluth separation at higher energies to determine G_E. As will be discussed below, using polarization measurements will allow a much more precise determination of G_E/G_M. JLab experiment 93-027 [9], which ran during the summer of 1998, has made such a precision measurement of the ratio for the proton.

Needless to say, because G_E was not well known even for the proton at high Q^2, the question of its possible modification in the nuclear medium remains an open question.

2 Polarization

2.1 Formalism

The development of high intensity, high polarization, continuous electron beams has opened a new avenue for exploration of medium effects. For the free nucleon, the spin transfer can be written in terms of the form factors as[16]

$$I_0 P_L = \frac{E+E'}{m_p}\sqrt{\tau(1+\tau)}G_M^2 \tan^2(\theta/2)$$

$$I_0 P_T = -2\sqrt{\tau(1+\tau)}G_M G_E \tan(\theta/2)$$

$$I_0 = G_E^2 + \tau G_M^2[1+2(1+\tau)\tan^2(\theta/2)]$$

$$\tau = Q^2/4m_p^2,$$

where E and E' are the energies of the incident and scattered electron, θ is the electron scattering angle, m_p is the proton mass, P_L is the polarization of the scattered proton in the direction of its momentum, P_T is the polarization transverse to the momentum and in the scattering plane. The ratio of the transferred polarizations is then

$$\frac{P_T}{P_L} = \frac{-2m_p}{(E+E')\tan(\theta/2)}\frac{G_E}{G_M}.$$

We use P_L and P_T to mean the polarization resulting from a 100% polarized beam. The actual polarizations are hP_L and hP_T, where h is the electron beam polarization, so both P_L and P_T change sign when the electron helicity changes sign.

Thus, the ratio of polarizations can be used to determine the ratio of the form factors without measuring an absolute cross section (although determination of the individual values of the form factors still requires knowledge of the cross section). The ratio is also independent of the beam polarization (assuming it is not zero) and of the analyzing power of the proton polarimeter. Because the measurement is made at a single angle, most systematic problems associated with absolute cross section measurements are eliminated. The integrated luminosity, spectrometer acceptance, and dead time are common and cancel in the ratio. The ratio also eliminates the kinematic factors which suppress G_E in the cross section measurement.

For nuclear targets the situation becomes more complicated. The ratio of polarizations is no longer determined only by the nucleon form factor. Nuclear effects change the observed polarization even if there are no changes in the form factors. The outgoing proton may interact with other nucleons. In addition, other effects, such as meson exhange currents, isobar configurations, or two body currents [10] may also change the recoil polarization. Calculation of these is model dependent and thus no completely unambiguous result can be determined. However, for certain kinematic settings calculations show that there is little model dependence and only small changes in the observed polarization[11].

The nuclear case also allows for an induced polarization normal to the scattering plane P_N. This polarization is due to the interaction of the scattered nucleon with the residual nucleus. Determination of this component allows for a check of how well a particular model describes the passage of the nucleon out of the nucleus. P_N is independent of the electron helicity, and thus is present even for an unpolarized electron beam.

2.2 Focal Plane Polarimeter

The JLab focal plane polarimeter was designed and built by a collaboration of Rutgers, William & Mary, Georgia, and Norfolk State, and funded by the U.S. National Science Foundation. The chamber design is based on one used for the EVA chamber at Brookhaven[12].

The polarimeter is mounted in the hadron spectrometer behind the spectrometer VDC's. It consists of four tracking straw chambers and a graphite analyzer. The chambers are numbered one to four with one the most upstream and four the most downstream. Each chamber is composed of six layers of straws. Chambers 1 and 2 have three V layers followed by three U layers and chamber 4 has three U layers followed by three V layers of straws, with U and V layers inclined at $\pm$ 45 ° with respect to the dispersive plane of the spectrometer. Chamber 3 has two U, two V, and two X layers. The X layer is horizontal and thus perpendicular to the dispersive plane of the spectrometer. In each set of U, V, X the individual planes are offset by half a straw from one plane to the next. The active areas of the chambers are: 1 - 60 x 209 cm, 2 - 60 x 209 cm, 3 - 124 x 272 cm, 4 - 142 x 295 cm.

Each straw is formed from a tube consisting of two layers of 50 μm thick mylar with an inner surface of 10 μm Al foil. The inner diameter is 1.044 cm. Each tube has a single wire of 25 μm diameter gold plated tungsten-rhenium strung down the center. The wires are held under a tension of about 60 g. The assembly holding the wire locates it at the center with an uncertainty of about +/- 75 μm. The center-to-center spacing of the wires is 1.095 cm for chambers 1 and 2, and 1.0795 cm for chambers 3 and 4.

The gas mixture used is 60/40 argon/ethane. The gas system has a combination of parallel and serial connections, depending on the chamber and orientation of the straws. In all cases, the efficiency of the individual straws is greater than 97%.

The total number of straws in the FPP is about 5200. In order to reduce the electronics required, sets of 8 straws are multiplexed. Each wire in a group of 8 has an individual discriminator which produces a fixed width for each wire, varying from 25 to 105 ns in each set of eight. Logic levels at the chamber are reduced to 10% of ECL levels to reduce noise and cross talk, and amplified to ECL levels just prior to the TDC's. These are sent to a multi-hit TDC which measures the start time and stop time. The wire hit is then determined from the start-stop difference and the drift time determined from the start time. The effective spatial resolution of the straws is about 250 μm.

The graphite analyzer consists of five sets graphite plates with two plates, left and right, in each set. Each plate has an area of 41.6 x 234 cm. The plates are beveled at an angle of 45° on the inner face so that the plates overlap when pushed together. The two plates can be independently pushed in or out of the active area. The thicknesses of the plates are 1.9, 3.8, 7.6, 15.2, and 22.9 cm. The density is 1.70 g/cm^3, giving mass thicknesses of 3.2, 6.5, 13.0, 25.9, and 38.9 g/cm^2.

The thickness of the analyzer is chosen to maximize the figure of merit. The statistical uncertainty on the measured polarization is proportional to $1\sqrt{A^2N}$, where A is the average analyzing power and N the number of scattered particles. A^2N is usually called the figure of merit. The analyz-

ing power peaks near a proton energy of 200 MeV, then drops for increasing energy. Fig. 1 shows the approximate proton-carbon analyzing power as a function of energy, based on parameterizations from several previous measurements[13, 14] As the proton energy increases the thickness of the analyzer can be increased, so the figure of merit does not decrease as fast with increasing energy as one might expect from the decreasing analyzing power. An estimated figure of merit is shown in Fig. 2. The fraction of protons incident on the analyzer which scatter between 5° and 20°, is estimated from previous measurements [14] and preliminary results of the FPP calibration done in 1998[15]. The vertical scale is of A^2 times the estimated percentage of incident protons scattered, integrated between 5° and 20°. This estimate is presented to indicate that the FPP may be used to higher energies with reasonable efficiency. A consistent set of analyzing powers and figures of merit for the FPP will be one result of JLab experiment 93-027[9].

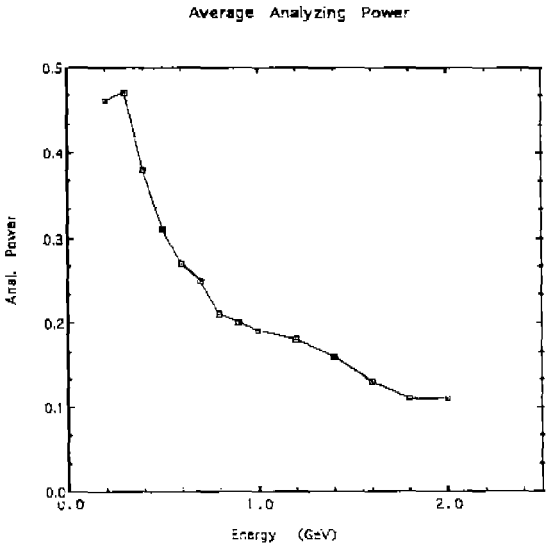

Fig. 1. Average analyzing power as a function of proton energy, for protons scattering between 5° and 20°[13, 14].

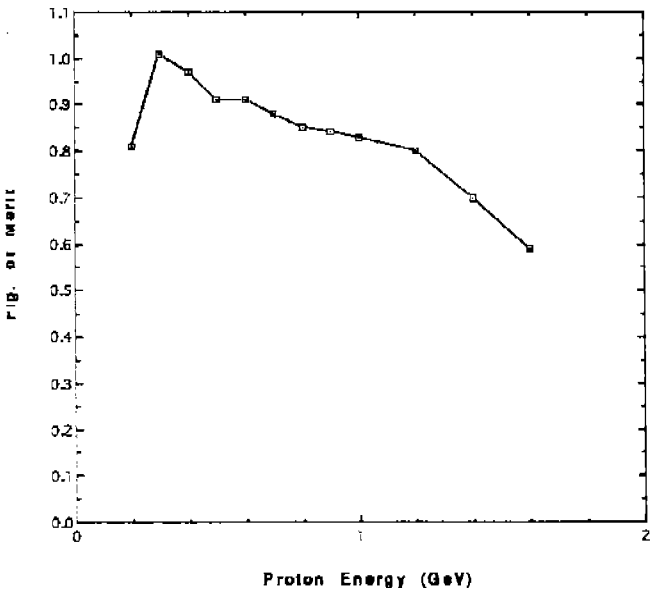

Fig. 2. Relative figure of merit as a function of proton energy. The vertical scale is A^2 times the estimated percentage of protons scattered between 5° and 20°. Graphite thicknesses used for this calculation were: 7.6 cm (200-300 MeV), 11.4 cm (400 MeV), 15.2 cm (500 MeV), 22.9 cm (600-700 MeV), 30.5 cm (800 MeV), 38.1 cm (900 MeV), and 51.4 cm (1000 MeV and greater)[14, 15].

2.3 Measurement of Polarization

The measurement of the polarization of intermediate energy protons is done by taking advantage of the substantial left-right scattering asymmetry present when transversely polarized protons scatter from various nuclear targets. There is no scattering asymmetry due to the longitudinal polarization, so only transverse polarizations can be measured. Graphite is the most commonly used analyzer, mainly because of its low cost and ease of handling.

The scattering cross section is given by

$$I(\theta,\phi) = I_0(\theta)[1 + A(\theta)P_n cos(\phi) + A(\theta)P_t sin(\phi)]$$

where θ is the polar scattering angle in the analyzer, ϕ is the azimuthal scattering angle, A(θ) is the analyzing power and P_n and P_t are the proton polarization in two orthogonal directions. We will use lower case subscripts

to indicate polarizations at the FPP and upper case to indicate polarizations at the target. The products AP_n, AP_t (which we will call ϵ_n and ϵ_t) can be extracted by a Fourier analysis of the scattered proton's azimuthal distribution[18]. If the analyzing power is known, the polarization can be determined.

In order to correctly extract $\epsilon_{n,t}$, the detection probability of the scattered proton must be equal for a given angle ϕ and $\phi+\pi$. Usually one requires that the scattering cone of all possible values of ϕ be detectable - the "cone test". The JLab FPP is sufficently large to ensure that nearly all scatters pass the cone test, as shown in Fig. 3.

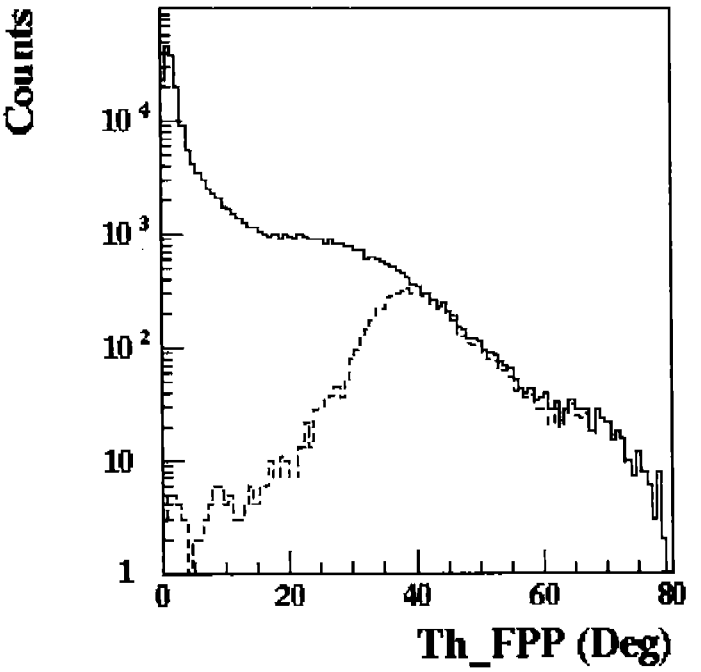

Fig. 3. FPP scattering angle distribution. The vertical scale is counts, the horizontal scale is the scattering angle in the analyzer in degrees. The dashed line indicates those events which did not pass the cone test.

The uncertainty on the asymmetry is given by

$$\sigma_\epsilon = \sqrt{\frac{2}{N}(1-\epsilon^2/2)}.$$

In practice ϵ is usually sufficiently small that σ can be estimated as $\sqrt{2/N}$.

2.4 Spin Precession

The proton polarization measured at the FPP is not the same as at the target due to the spin precession in the magnetic spectrometer. The precession can be described by the spin transport matrix

$$\begin{pmatrix} a_{11} & a_{12} & a_{13} \\ a_{21} & a_{22} & a_{23} \\ a_{31} & a_{32} & a_{33} \end{pmatrix} \begin{pmatrix} P_N \\ P_L \\ P_T \end{pmatrix} = \begin{pmatrix} P_n \\ P_l \\ P_t \end{pmatrix}.$$

The a_{ij} are functions of the proton momentum, and the position and angle at which the proton enters the spectrometer. $P_{N,L,T}$ are the spin components at the target, with N normal to the scattering plane, L in the momentum direction, and S transverse to the momentum and in the scattering plane, and $P_{n,l,t}$ are the spin components at the polarimeter.

For the case of a single proton momentum, pure dipole field, and constant entry point and angle, the matrix simplifies to

$$\begin{pmatrix} cos(\chi) & -sin(\chi) & 0 \\ sin(\chi) & cos(\chi) & 0 \\ 0 & 0 & 1 \end{pmatrix} \begin{pmatrix} P_N \\ P_L \\ P_T \end{pmatrix} = \begin{pmatrix} P_n \\ P_l \\ P_t \end{pmatrix},$$

where χ is the precession angle for a simple dipole field.

The inverse matrix can be determined, but the measured polarizations can be transformed to the target polarizations only if all three polarization components are measured. Because P_l cannot be measured with the FPP, another method must be used. An iterative technique has been developed[19]; the results presented here are based on the simple dipole approximation. Details will be presented at a later date.

3 Experiment 89-033

Experiment 89-033[17] was a measurement of induced and transferred polarization in the reaction $^{16}O(\vec{e}, e'\vec{p})^{15}N$. It was the first experiment at JLab to use a polarized electron beam and the first to use the FPP.

The beam energy was 2.445 GeV with a polarization of about 35%, the electron scattering angle was 23.4° and the central scattered electron energy was 2.000 GeV, the quasi-elastic peak. The central proton momentum was 973 MeV/c. The recoil proton was detected in quasi-perpendicular kinematics at angles of 50.8°, 53.3°, 55.7°, 60.5°, corresponding to missing momenta of -85, 0, 85, and 140 MeV/c. Positive missing momentum corresponds to the case where the missing momentum vector points to smaller scattering angles on the proton side. Elastic hydrogen scattering can be seen at spectrometer angles of 53.3° and 55.7°.

The target was a waterfall consisting of three foils with a total thickness of about 0.5 g/cm^2, as shown in Fig. 4. The use of three separated foils allowed sufficient energy resolution to distinguish the $p_{1/2}$ ground state of ^{15}N from the first excited state $p_{3/2}$, and the $s_{1/2}$ shell as shown in Fig. 5. The boundaries for the shells are set as 10-17 MeV, 17-28 MeV, and 28-50 MeV.

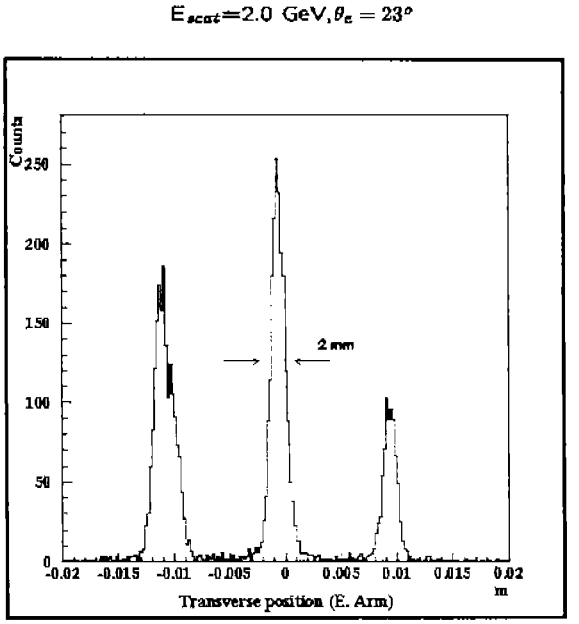

Fig. 4. Target projection, showing the three water foils.

The polarization of the outgoing proton is measured for each helicity state. By subtracting the two, the polarizations P_L and P_T can be found, while the sum gives P_N. All components were found for both ^{16}O and hydrogen (where P_N is zero), with a preliminary result for hydrogen shown in Fig. 6. Measurements of scattering from hydrogen reveal an instrumental asymmetry of about 0.006; with the carbon analyzing power of about 0.4; this yields a polarization of 1.5%. This extremely small value indicates that high statistics measurements of induced polarization can be made reliably.

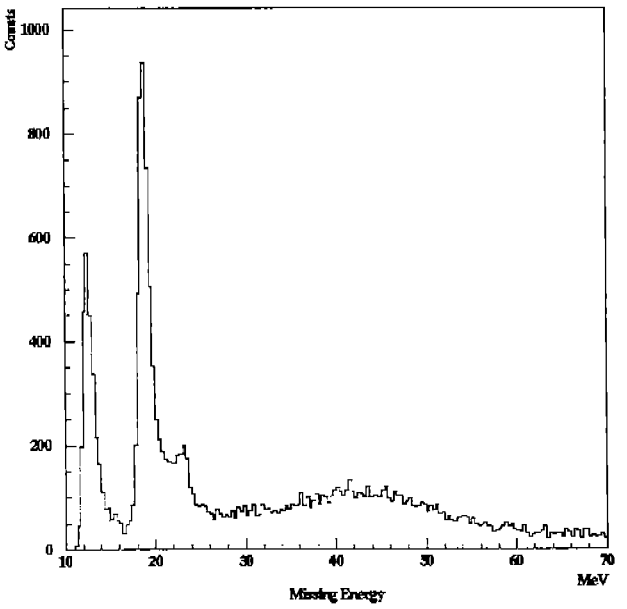

Fig. 5. The missing energy, defined as the beam energy minus the sum of the measured energies of the scattered electron and proton and calculated kinetic energy of the recoil nucleus.

Because we know conventional nuclear effects change the values of P_L and P_T, one cannot simply take the ratio to find G_E/G_M as is done on hydrogen. In order to account for this, we have used J. Kelly's code LEA [11] to calculate the expected value of P_T/P_L. The observed P_T/P_L is divided by the LEA predicted ratio to determine the form factor ratio in the nucleus.

As of this writing, we are still studying the spin transport of the spectrometer, which precludes us from making a firm statement on the observed value of P_T/P_L. The statistical uncertainty for individual states is too large for a meaningful result, so we have combined all states and all missing momentum measurements. Using the pure dipole approximation for spin transport, our preliminary result for the super-ratio of experiment to theory, is 1.07 ± 0.09 for $(P_T/P_L)_{expt}/(P_T/P_L)_{theory}$. This is expected to be 1.0 if the nucleon is unchanged and all nuclear effects are accounted for.

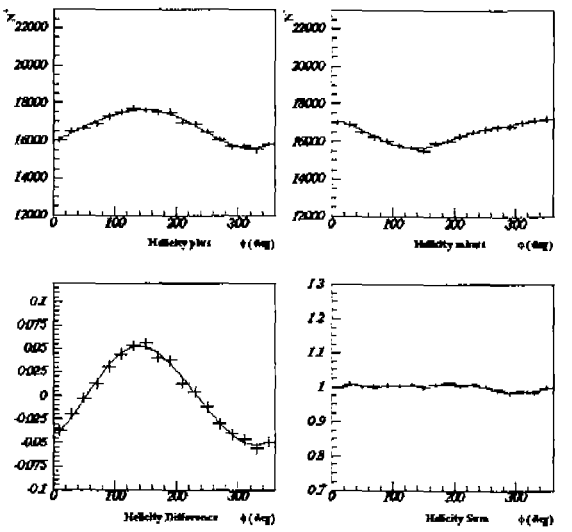

Fig. 6. Azimuthal asymmetery for helicity sum and difference for hydrogen.

4 Future Prospects

The good performance of the FPP has shown that high precision polarization measurements can be made given enough time. The question of the best kinematics and target nucleus to study remains to be answered. The Adelaide group has recently presented new calculations of both the free nucleon form factors and the in-medium form factors [20, 21, 22]. Their model gives a good description of the free nucleon form factors. Using the quark meson coupling model (QMC), they calculate expected modifications of the form factors in the nuclear medium. The model has two very interesting predictions. First, the magnetic form factor changes by only a few percent for a Q^2 of 0.8 $(GeV/c)^2$, while the electric form factor changes by about 10% to 15%, so the ratio of G_E/G_M is predicted to be 10-15% smaller than the free value. The effect becomes more pronounced at higher Q^2 and the ratio is predicted to be 15-20% smaller at Q^2 of 2.5 $(GeV/c)^2$. Secondly, they predict that the change in the form factor is almost as strong in ^{4}He as in ^{16}O, and indeed, that there is little A dependence. The FPP is capable of making measurements

of the P_T/P_L ratio at level of a few percent, giving a strong incentive to proceed with high statistics measurements on ^{4}He as well as heavier nuclei and at higher Q^2.

5 Conclusions

The first measurements of $(\vec{e}, e'\vec{p})$ polarization transfer on a nucleus heavier than deuterium have been performed. The JLab FPP was successfully commissioned. The good performance of the FPP shows the feasibility of performing high precision measurements of the G_E/G_M ratio of a nucleon in the nuclear medium.

6 Acknowledgments

We would like to thank the staff at TJNAF for dedicated support of the experimental program. The author would like to acknowledge the efforts of the 89-033 core group: F.T. Baker, L. Bimbot, E. Brash, C.C. Chang, D. Dale, J.M. Finn, K. Fissum, A. Gasparian, R. Gilman, C. Glashausser, J. Gao, M. Jones, J. Kelly, G. Kumbartzki, N. Liyanage, J. McIntyre, R. van der Meer, S. Nanda, C. Perdrisat, V. Punjabi, P. Rutt, D. Zainea, and especially the thesis students associated with the FPP experiments, S. Malov, G. Quéméner, and K. Wijesooriya. This work is supported in part by the U.S. National Science Foundation and the U.S. Dept. of Energy.

References

1. P.K.A. de Witt Huberts, AIP Conf. Proc. **269**, 344 (1993).
2. W. Bertozzi, R.W. Lourie, and E.J. Moniz, in Modern Topics in Electron Scattering, p. 419, B. Frois and I. Sick, eds., World Scientific, 1991.
3. X. Song et al., Z. Phys. A **341** 275 (1992).
4. J. Jourdan, Phys. Lett. **B353**, 189 (1995).
5. J. Jourdan, Nucl. Phys. **A603**, 117 (1996).
6. D.B. Day et al., Phys. Rev. Lett., **59**, 427 (1987).
7. D.B. Day et al., Ann. Rev. Nucl. Sci. **40**, 357 (1990).
8. J. Arrington et al., Phys. Rev. C **53**, 2248 (1996).
9. Electric Form Factor of the Proton by Recoil Polarization, C.F. Perdrisat, V. Punjabi, and M. Jones, spokespersons.
10. S. Boffi, et al., Nucl. Phys. **A539**, 597 (1992), S. Boffi et al., Nucl. Phys. **A518**, 639 (1990).
11. J.J. Kelly Phys. Rev. C **56**, 2672 (1997), and Adv. in Nucl. Phys. **23**, 75 (1996).
12. M. Kmit, Brookhaven Informal Report EP&S 91-4.
13. M. McNaughton et al., NIM **A241**, 435 (1985), E. Aprile-Giboni, NIM **215**, 147 (1983), N.E. Cheung et al., NIM **A363**, 561 (1995).
14. B. Bonin et al., NIM **A288**, 379 (1990).

15. A. Besson, FPP group internal report.
16. R.G. Arnold et al., Phys. Rev. C **23**, 363 (1981).
17. Spokespersons: C. Glashausser, C.C. Chang, S. Nanda, P. Rutt.
18. D. Besset et al., Nucl. Inst. Meth. **166**, 515 (1979).
19. G. Quéméner and C. F. Perdrisat, private communication.
20. D. H. Lu et al., Nucl. Phys. **A634**, 443 (1998).
21. D. H. Lu et al., Phys. Lett. **B417**, 217 (1998).
22. D. H. Lu et al., Phys. Rev. C **55**, 2628 (1998).